Tellus (1985), *37A*, 258–275

On the time variation in the tropical energetics of large-scale motions during the FGGE summer

TSING-CHANG CHEN, *Department of Earth Sciences, Iowa State University, Ames, IA 50011, USA*

(Manuscript received February 2; in final form October 15, 1984)

ABSTRACT

A pronounced quasi-periodic variation with a period of $1\frac{1}{2}$ months (OHM) was observed in the tropical (10° S–20° N) energetics during the FGGE summer using the data generated by the FGGE III-b analyses of the European Center for Medium-Range Weather Forecasts. This quasi-periodic variation in the tropical energetics was found to be mainly attributed to wave 1. The time evolution in the three-dimensional structure and dynamical transport processes of this wave are used to explore how this OHM variation occurred and was maintained. It was revealed that the OHM variation in the eddy-available potential energy essentially occurs north of the equator and in the eddy kinetic energy appears both north and south of the equator. The former variation is possibly supported by the generation of the eddy-available potential energy and the latter variation north of the equator is maintained by the release of the eddy-available potential energy due to the thermally direct overturnings. The OHM variation in the eddy kinetic energy south of the equator is sustained by the barotropic interaction between the zonal flow and wave 1. A possible mechanism to induce the OHM variation in the tropical energetics is also discussed.

1. Introduction

Our understanding of the large-scale circulation and dynamics in the tropical upper troposphere has advanced significantly in the past decade. Several energetics studies (Kanamitsu et al., 1971; Depradine, 1980; Chen, 1980; 1983; Chen and Marshall, 1984) were carried out in order to explore the maintenance of the large-scale motions in the tropics. It is found that the energetics of the tropical atmosphere differ considerably from those of the midlatitude atmosphere. In midlatitudes, the unstable baroclinic waves of medium scale are essential agents to release the available potential energy. In contrast, the planetary waves, induced by the east-west land-sea contrast, are the most important energetic scale of atmospheric motions in the tropics.

The above arguments are based upon the seasonal mean analysis of atmospheric energetics. In fact, the atmospheric energetics vary significantly in time. Some quasi-periodic time variations of atmospheric energetics, for instance, annual variation (Wiin-Nielsen, 1967; Chen and Buja, 1983) and vacillation (e.g. Hunt, 1978; Chen and Marshall, 1984) are very well-known phenomena in meteorology. The former variation is essential to the climate simulation (Sela and Wiin-Nielsen, 1971), while the latter variation is important to the medium-range forecast (Hunt, 1978). A great deal of effort has been made to explore mechanisms stimulating these quasi-periodic variations of atmospheric energetics. The annual variation of atmospheric energetics is attributed to the annual change of the north–south differential heating, but the vacillation of atmospheric energetics is still not fully understood.

However, these studies dealing with the quasi-periodic time variations of atmospheric energetics are mainly concerned with the atmospheric circulation and weather system in midlatitudes. Although the atmospheric energetics of large-scale motions in the tropics differ from those in midlatitudes, one may wonder whether a similar or a different type of time variation of atmospheric energetics, as described above, possibly exists in the tropics. Using the data generated by the FGGE III-b analyses of the European Center for Medium

Range Weather Forecasts, we find that the tropical atmospheric energetics exhibit a pronounced quasi-periodic variation with a period about $1\frac{1}{2}$ months (OHM) during the FGGE summer. The understanding of the stimulation and maintenance of this quasi-periodic OHM variation may be helpful to the long-range weather forecasts or the short-term climate prediction in the tropics. To reach this goal, the time evolution in the synoptic structure and dynamical transport properties of ultralong waves in tropics are examined. Since it is also found that wave 1 dominates this OHM variation in the tropical energetics, we focus our effort on this wave to facilitate the search for the physical processes maintaining this quasi-periodic variation and the possible mechanism responsible for it.

The energetics scheme, illustrations of wave-1 structure and transport properties, and data used are described in Section 2. The time evolution of tropical energetics in the FGGE summer is presented in Section 3. The synoptic structure of wave 1 in various phases of time variation in the tropical energetics is shown in Section 4. The time evolution of dynamical transport properties of wave 1 is discussed in Section 5 to illustrate how the quasi-periodic variation of the tropical energetics is maintained. Concluding remarks and discussion are provided in Section 6.

2. Computation scheme and data

The spectral energetics scheme proposed by Saltzman (1957) is used in the present study to examine the maintenance of ultralong waves in the tropics. The spectral forms of energy equations can be expressed as,

$$\frac{\mathrm{d}K_Z}{\mathrm{d}t} = \sum_{n=1}^{N} C(K_n, K_Z) + C(A_Z, K_Z)\, B(\phi_Z) + B(K_Z) + NF(K_Z) - D(K_Z), \tag{1}$$

$$\frac{\mathrm{d}K_n}{\mathrm{d}t} = -C(K_n, K_Z) + CK(n/m, l) + C(A_n, K_n), + B(\phi_n) + B(K_n) + NF(K_n) - D(K_n), \tag{2}$$

$$\frac{\mathrm{d}A_Z}{\mathrm{d}t} = -\sum_{n=1}^{N} C(A_Z, A_n) - C(A_Z, K_Z)\quad B(A_Z) + NF(A_Z) + G(A_Z), \tag{3}$$

$$\frac{\mathrm{d}A_n}{\mathrm{d}t} = C(A_Z, A_n) - C(A_n, K_n) + CA(n/m, l) + B(A_n) + NF(A_n) + G(A_n). \tag{4}$$

The notations used here are conventional. $CX(n/m,\ l)$ is the rate of change of quantity X at wavenumber n due to triplet interactions between all possible combinations of m and l with n. $B(\ )$s are boundary fluxes of energy variables ( ) and $NF(\ )$s are boundary fluxes of ( ) due to triplet interactions among waves. $G(A)$ and $D(K)$ are generation of available potential energy and dissipation of kinetic energy, respectively. Note that, in the eddy energies,

$$K_E = \sum_{n=1}^{N} K_n \quad \text{and} \quad A_E = \sum_{n=1}^{N} A_n,$$

and in the energy conversions,

$$C(A_Z, A_E) = \sum_{n=1}^{N} C(A_Z, A_n) \quad \text{and} \quad C(K_E, K_Z) = \sum_{n=1}^{N} C(K_n, K_Z).$$

Therefore, K_E and A_E equations can be obtained by summing eqs. (2) and (4) to form the traditional Lorenz energy cycle with eqs. (1) and (2).

The horizontal (longitude–latitude) charts and longitude-pressure cross sections of temperature and zonal motion at a given latitude are employed to show the three-dimensional structure of ultralong waves, essentially wave 1 in the tropics. These two meteorological variables will be subsequently used in the energetics analysis. The vertical transport of sensible heat and the horizontal transport of momentum by wave 1 are also displayed in the same manner as the synoptic structure of this wave is presented. The synoptic structure and dynamical transport properties of wave 1 will be used to illustrate the local maintenance of the quasi-periodic OHM variation in the tropical energetics and to shed light on the possible cause of this phenomenon.

The data generated by the ECMWF FGGE III-b analyses (Bengtsson et al., 1982) for the FGGE summer at the mandatory levels are used in this study. However, some deficiencies of data have been found in these analyses. The vertical velocities are severely underestimated throughout the equatorial regions. The kinematic method with

O'Brien's (1970) adjustment scheme was adopted to evaluate the vertical velocities. The boundary conditions of $\omega = 0$ at $p = 0$ mb and 1000 mb are imposed. The temperatures were also re-created following the procedures suggested in the World Data Center-A(WDC-A) FGGE Data Catalog published by the National Climatic Center, USA. The static stability, which used the tropical area-mean (10° S–20° N) temperature, is calculated at every synoptic time. The computational domain extends from 10° S to 20° N. The spectral energetics include 18 wave components.

3. Time variation of tropical energetics

3.1. Energies

In order to examine the time variation in the energetics of large-scale motions in the tropics during the FGGE summer, time series of both zonal and eddy components of available potential and kinetic energies, A_Z, A_E, K_Z, and K_E, are displayed in Figs. 1 and 2, respectively. The spline curve fit is applied to the time series of the energy variables in such a way that the major long-period (compared to the entire summer) variation can be visualized easily. It is found that both the eddy-available potential and the eddy kinetic energy exhibit a pronounced bimodal variation in time over the entire FGGE summer. The time span from one minimum (maximum) value of the eddy energies to another one is about $1\frac{1}{2}$ months. Time variations of A_E and K_E are more-or-less in phase. In contrast, both the zonal available potential energy and the zonal kinetic energy have only one major maximum over the entire FGGE summer. Time variations of zonal energies are out of phase with those of eddy energies.

Table 1. *Ratios between the maximum energy changes due to the quasi-periodic OHM variation in 1979 summer and the summer mean energies*

	A_Z	K_Z	A_E	K_E
Summer mean (10^3 J m^{-2})	14·8	97·1	59·2	228·4
ratio	100%	80%	50%	70%
	$\Delta A_Z/A_Z$	$\Delta K_Z/K_Z$	$\Delta A_Z/A_E$	$\Delta K_E/K_E$

It is shown in Table 1 that the magnitudes of zonal energies (A_Z or K_Z) are generally several factors smaller than those of their corresponding eddy energies (A_E or K_E). However, the correlation between time variations of zonal and eddy energies in the tropics is an interesting situation, similar to the vacillation of atmospheric energetics in midlatitudes, except that the latter has a shorter period (2–4 weeks). The % of the maximum energy changes (ΔA_Z, ΔA_E, ΔK_Z, ΔK_E) in the quasi-periodic OHM variation compared with the summer mean energies in the FGGE summer is also shown in Table 1. This table provides a quantitative indication of the significance of the magnitude changes in the various types of energies in this quasi-periodic variation of tropical energetics.

It was revealed in our previous studies that wave 1 dominates the energy spectra of both available potential and kinetic energies in the tropics and contributes about 30% and 35% to the respective eddy energies of both types. It may be expected that wave 1 is also an important contributor to the OHM variation of eddy-available potential and kinetic energy. Time series for the energies of wave 1 (A_1 and K_1) and energies of shorter waves ($\sum_{n=2}^{18} A_n$ and $\sum_{n=2}^{18} K_n$) are also displayed in Figs. 1 and 2. Although the seasonal mean values of $\sum_{n=2}^{18} A_n$ and $\sum_{n=2}^{18} K_n$ are much larger than those of A_1 and K_1, respectively, it is evident from Figs. 1 and 2 that wave 1 is the major component describing the quasi-periodic OHM variation of eddy energies. The contrast between the time variation of the energies of wave 1 and the shorter waves provides us with a simplification for the search for the possible mechanism inducing the quasi-periodic OHM variation of eddy energies. Therefore, we focus our attention on wave-number 1.

3.2. Energy conversion

We shall examine time variations of various energy conversions to understand how the time variations of various energies are maintained. In order to facilitate the discussion on the correlations between them, it is informative to provide a brief summary of the summer-mean energetics of the tropical (10° S–20° N) troposphere from our previous studies (Chen and Marshall, 1984). The overall feature of the tropical energy cycle over the entire troposphere is similar to the upper troposphere summarized by Krishnamurti (1979).

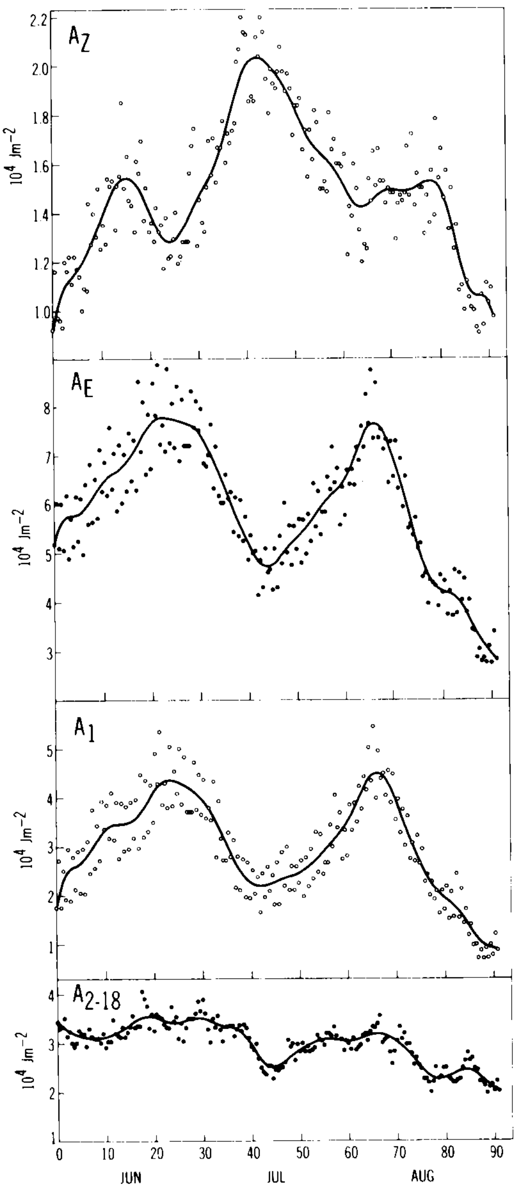

Fig. 1. Time series of available potential energy: (a) (A_Z), (b) eddy (A_E), (c) wave 1 (A_1) and (d) waves 2 to 18 (A_{2-18}).

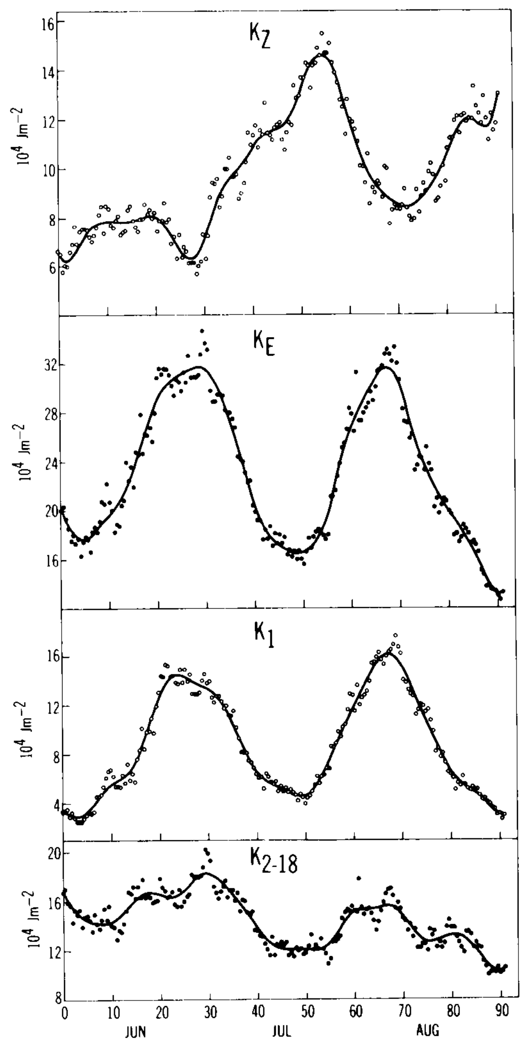

Fig. 2. Same as Fig. 1 except for kinetic energy (K).

Two types of energy conversions are shown in the Lorenz energy cycle: (a) the release of zonal and eddy available potential energy, $C(A_Z, K_Z)$ and $C(A_E, K_E)$, and (b) the exchange of energy between zonal and eddy flows, $C(A_Z, A_E)$ and $C(K_E, K_Z)$. The contrast in magnitudes between these two types of energy conversion shows that the release of zonal and eddy-available potential energy are the major energy conversions in the tropics. In other words, the available potential energy generated by the diabatic heating is converted to kinetic energy through the thermally direct overturnings in order to maintain the zonal and eddy motions. It was found that 64% of the release of eddy-available potential energy is contributed by wave 1, $C(A_1, K_1)$. The non-linear interaction transfers the available potential energy from small waves to

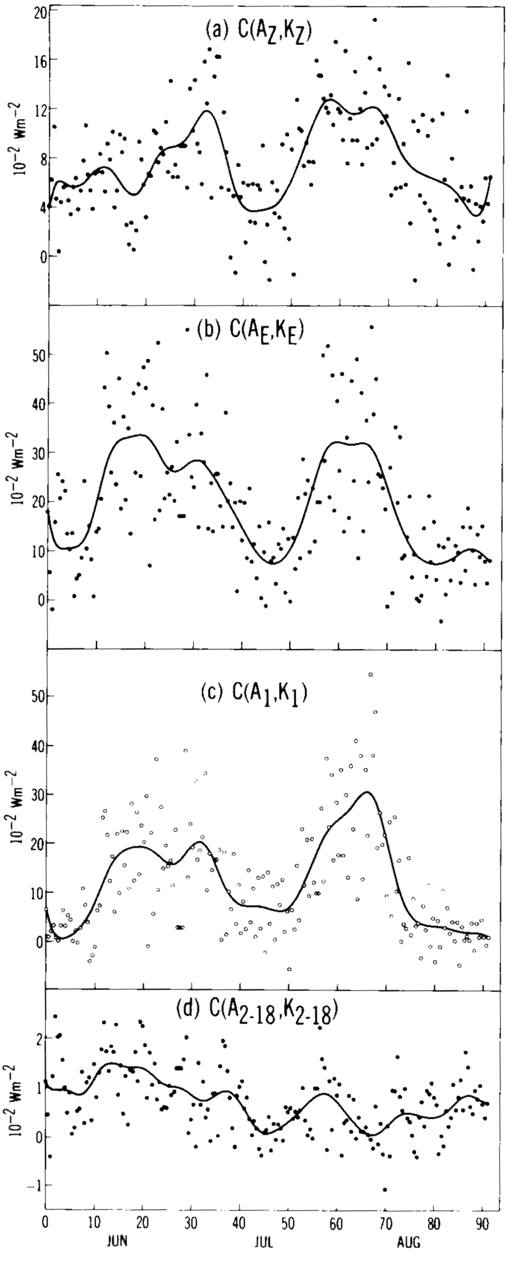

Fig. 3. Time series of (a) $C(A_Z, K_Z)$, (b) $C(A_E, K_E)$, (c) $C(A_1, K_1)$ and (d) (A_{2-18}, K_{1Z}).

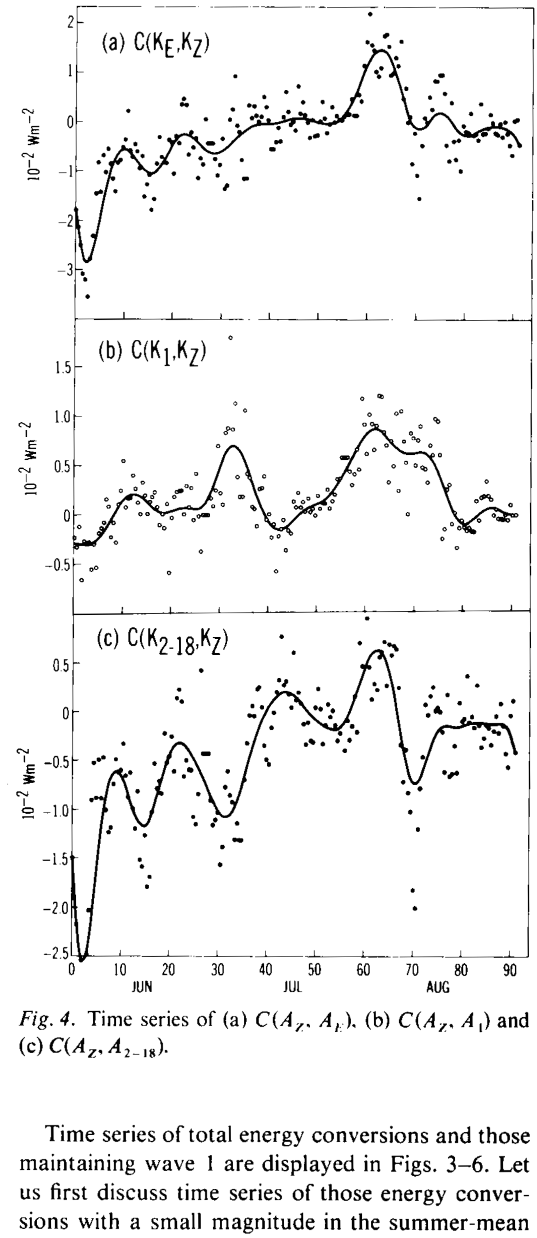

Fig. 4. Time series of (a) $C(A_Z, A_E)$, (b) $C(A_Z, A_1)$ and (c) $C(A_Z, A_{2-18})$.

ultralong waves, but oppositely transfers the kinetic energy from ultralong waves to short waves. However, the non-linear transfers are small in magnitude.

Time series of total energy conversions and those maintaining wave 1 are displayed in Figs. 3–6. Let us first discuss time series of those energy conversions with a small magnitude in the summer-mean energy cycle. The energy exchanges between the zonal and eddy flows (Figs. 3 and 5) do not show any obvious trend of a quasi-periodic OHM variation. It seems to indicate that these energy conversions do not support this quasi-periodic OHM variation of eddy energies. Surprisingly, the contributions of wave 1 to the kinetic energy exchange between zonal and eddy flows exhibit a bimodal variation in time which matches the

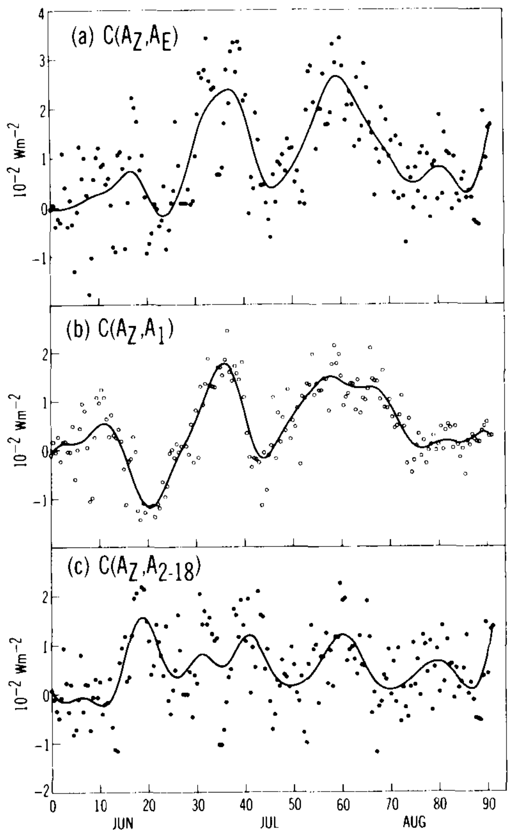

Fig. 5. Time series of (a) $C(K_l, K_Z)$, (b) $C(K_1, K_Z)$, and (c) (K_{2-18}, K_Z).

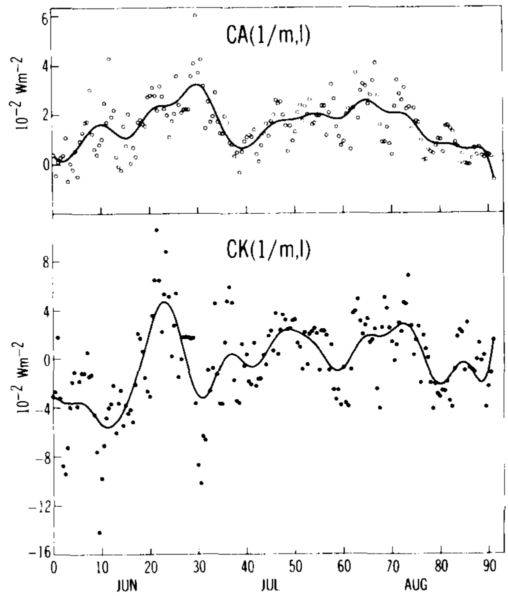

Fig. 6. Time series of (a) $CA(1/m, l)$ and (b) $CK(1/m, l)$.

quasi-periodic OHM variation of eddy energies. Although the magnitude of this energy conversion by wave 1 is small, it may play a significant rôle in maintaining the OHM variation and will be illustrated later. The non-linear transfer (Fig. 6) obviously furnishes the available potential energy to wave 1 from the smaller waves, but serves to build, then dissipate, the kinetic energy of wave 1. The former process does display a bimodal variation over the FGGE summer, but not the latter process. Because of their small magnitude, the non-linear transfers of energy are not important in maintaining the OHM variation in energies of wave 1.

Time series of the release of zonal and eddy-available potential energy due to thermally direct overturnings (Fig. 4) exhibit a pronounced bimodal variation over the FGGE summer. These two energy conversions are not only significant in the summer-mean energy cycle, but also important in maintaining the OHM variation of eddy energies. Recall that zonal energies (A_Z and K_Z) have only one major maximum value in the tropics during this summer when eddy energies (A_E and K_E) are at a minimum. It is surprising to reveal that the release of zonal available potential energy by the Hadley-type overturning possesses a bimodal variation over this FGGE summer. It indicates that the conversion of zonal available potential energy to zonal kinetic energy is minimal when the mean zonal circulation reaches its maximum intensity. The correlation between the zonal energies and this energy conversion in the OHM variation of the tropical atmospheric energetics differs from that in the vacillation of the midlatitude atmospheric energetics. Furthermore, it was mentioned previously that wave 1 contributes significantly to the summer-mean value of the release of eddy-available potential energy. However, the contrast between the time series of the contribution by wave 1 and the time series of the other waves to the release of eddy-available potential energy shows evidently that wave 1 is responsible for this OHM variation.

It is inferred from the summer-mean energy cycle that the generation of zonal and eddy-available potential energy, $G(A_Z)$ and $G(A_E)$, by diabatic heating, provides the source of these two types of energies, which are later released by the thermally direct overturnings. However, one may question whether $G(A_Z)$ and $G(A_E)$ also possess a quasi-periodic OHM variation in the FGGE summer in order to maintain this variation of the release of available potential energy. As is well-known, the computations of both $G(A_Z)$ and $G(A_E)$ involve the evaluation of diabatic heating in the tropics which cannot be directly calculated. At any rate, this comment suggests a further step which we should pursue in the future.

4. Time evolution in structure of wave 1

In this section we focus on the time evolution in the structure of wave 1. The available potential energy depends on the temperature, while the kinetic energy of the summer tropical atmosphere is mostly decided by the zonal motion. Therefore, we select the temperature and zonal wind of wave 1, T_1 and u_1, to serve our purpose here in concert with the time variation of energetics. Hovmöller (x–t) diagrams of T_1 and u_1 and latitude-time diagrams of the root-mean-square (rms) amplitude of these two quantities will be used to examine the mobility of wave 1 in the tropics. Horizontal charts at 200 mb and longitude-pressure cross sections at various latitudes will be used to illustrate the three-dimensional structure of wave 1 in various phases of the tropical energetics.

4.1. Hovmöller (x–t) and latitude-time diagrams

Madden and Julian (1971, 1972) and Yasunari (1979, 1980, 1981) have identified a 40–50 day oscillation in several meteorological variables. Note that these studies employ the time series analysis with statistical technique. Since the data set used in this study covers only 3 months (June, July, August), we can not obtain a significant confidence applying the statistical technique in the OHM variation analysis. In view of this limitation, a visual approach using the spectrally filtered (SF) Hovmöller and latitude-time diagrams of wave 1 will be utilized to illustrate the mobility of this wave.

The maximum amplitudes of temperature and zonal wind disturbances occur in the upper troposphere. The SF Hovmöller diagrams of T_1 and u_1 at 200 mb of two latitudes, 20° N, and 10° S, are displayed in Fig. 7. The reason for selecting 20° N and 10° S is because they are the north and south boundaries of our computational domain. It is observed that the thermal ridge is somewhat west of the monsoon and westward flow of wave 1 exists over the monsoon area north and south of the equator. It is discernible that wave 1 at 10° S is more mobile than that at 20° N. Madden and Julian, and Yasunari described the disturbances associated with the 40–50 day oscillation in the tropics as eastward propagating. Although wave 1 at 20° N seems to be quasi-stationary, it is not difficult to perceive the eastward movement of the transient mode of wave 1 by removing the seasonal mean values of T_1 and u_1. At 10° S, it is clear that wave 1 exhibits the tendency of eastward propagation, even without removing the seasonal mean value of T_1 and u_1. The amplitudes of u_1 are comparable in these two latitudes, while those of T_1 decrease southward. Nevertheless, the OHM variation of the T_1 and u_1 amplitudes is very obvious and the maximum amplitudes always occur in about the same longitudinal location. In other words, the amplification of wave 1 in the tropics has a preference of location. In addition, there seems to be another type of oscillation with a period of about a half month as suggested by Yasunari (1979) and Krishnamurti and Bhalme (1976).

Yasunari (1979, 1980, 1981) also showed that disturbances of the 40–50 day oscillation over the north Indian Ocean, in general, propagate northward from 10° S and decay at 20° N. In order to examine whether wave 1 possesses this propagation property, the latitude-time diagrams for the rms (root-mean-square) amplitudes of T_1 and u_1 over the entire FGGE summer at 200 mb are displayed in Fig. 8. It does not seem to indicate that wave 1 propagates northward; instead wave 1 is amplified at latitudes where the maximum amplitude of T_1 and u_1 appear. The SF Hovmöller and latitude-time diagrams of T_1 and u_1 show that the OHM variation in energies of wave 1 is essentially due to the amplification and decay of wave 1 at a preferable location.

4.2. Structure of wave 1

In order to obtain a better understanding of the characteristics of wave 1 in various phases of the

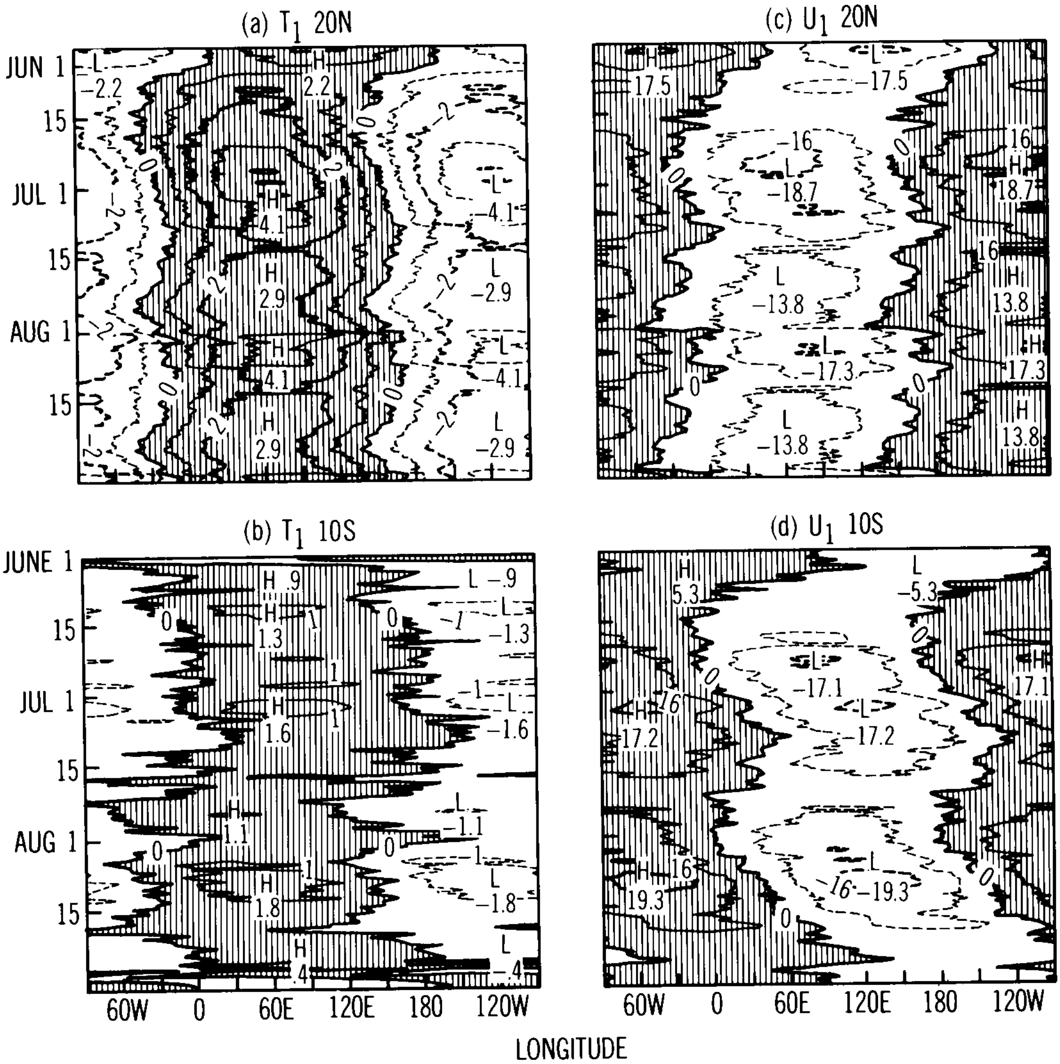

Fig. 7. Spectrally filtered Hovmöller diagrams for temperature of wave 1 (T_1) at (a) 20° N, (b) 10° S, and for zonal wind of wave 1 (u_1) at (c) 20° N, (d) 10° S. Units: degrees for T_1 and m s^{-1} for u_1.

eddy-energy variation, the 10-day averaged structure of temperature and zonal wind of wave 1 is examined. Referring to the time variation of eddy energies shown in Figs. 1 and 2, we select five 10-day periods which include 3 phases of minimum eddy energies and 2 phases of maximum eddy energies. These 5 phases are as follows: June 1–10 (minimum), June 21–30 (maximum), July 13–22 (minimum), August 1–10 (maximum) and August 22–31 (minimum.).

4.2.1. Temperature. The temperature structure of wave 1 (T_1) is depicted in Fig. 9. The summer-mean state is used as a reference to illustrate the time-variation of the wave structure. Let us first examine the horizontal structure at 200 mb. The summer-mean state (Fig. 9f) shows that the temperature amplitude of wave 1 north of the equator is larger than that found south of the equator, and is negligible in the vicinity of the equator. The thermal ridge or trough of wave 1 does not possess any significant tilting north of the equator, but displays a SE–NW tilting south of the

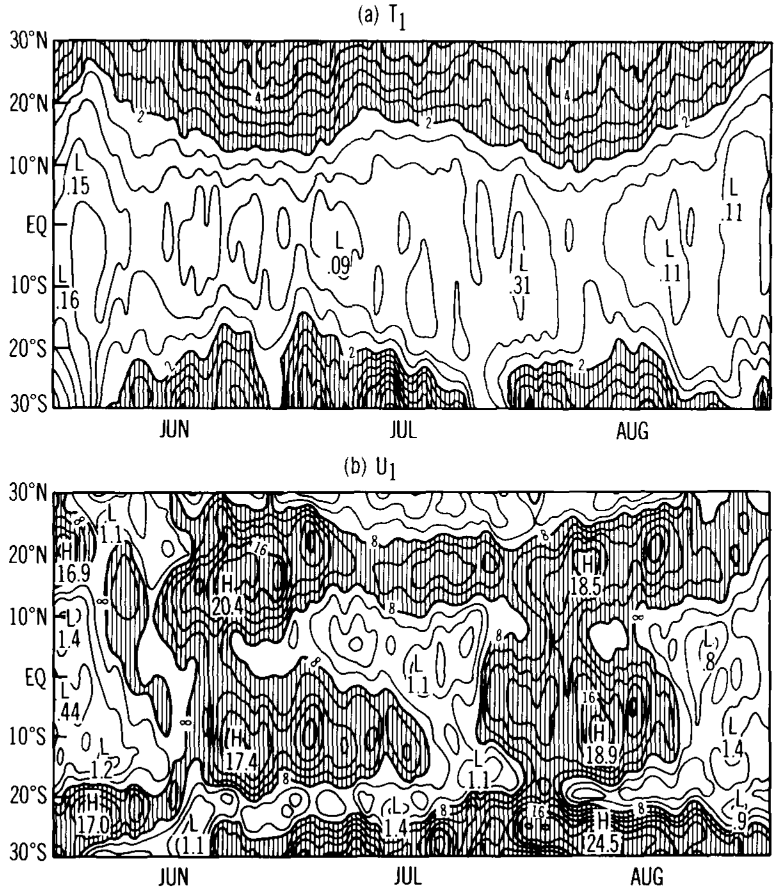

Fig. 8. Latitude-time diagrams for the root-mean-square (rms) amplitude of (a) temperature and (b) zonal motion of wave 1. Units: degrees for T_1 and m s^{-1} for u_1.

equator. During the various phases of the tropical energetics (Figs. 9a–e), the general feature of this wave is similar to the summer-mean structure, except in the first phase (June 1–10) which belongs to the preonset of monsoon. At this state, wave 1 is not well developed and its thermal ridge (or trough) tilts in the NE–SW direction north of 10° N. The available potential energy of wave 1 ($\sim T_1^2$) in our computational domain (10° S–20° N) mainly originates from the area north of the equator. The quasi-stationary location of thermal ridge over the monsoon area and the quasi-periodic variation of the temperature amplitude of wave 1 indicates that a heating source inducing the thermal ridge of this wave must also be located in the same location and varies in its intensity with a period of about $1\frac{1}{2}$ months. This conjecture of the heating location is based upon the satellite observation of rainfall (Rao and Theon, 1977) and clouds (Sadler, 1969).

According to the latitudinal distribution of wave 1 amplitude, we select 20° N to illustrate the vertical structure of this wave. The summer-mean temperature of wave 1 (Fig. 9) has its maximum amplitude at 200 and 850 mb. This indicates that a heating source generating the positive perturbation of temperature over the monsoon area has its maximum intensity in the upper and lower troposphere. This characterizes the stationary waves in the summer tropics (White, 1982). It should be mentioned that the temperature of wave 1 vertically changes its phase at 150 mb.

The vertical temperature structure in various phases (Fig. 9g–k) of the tropical energetics also has a general feature similar to the summer-mean

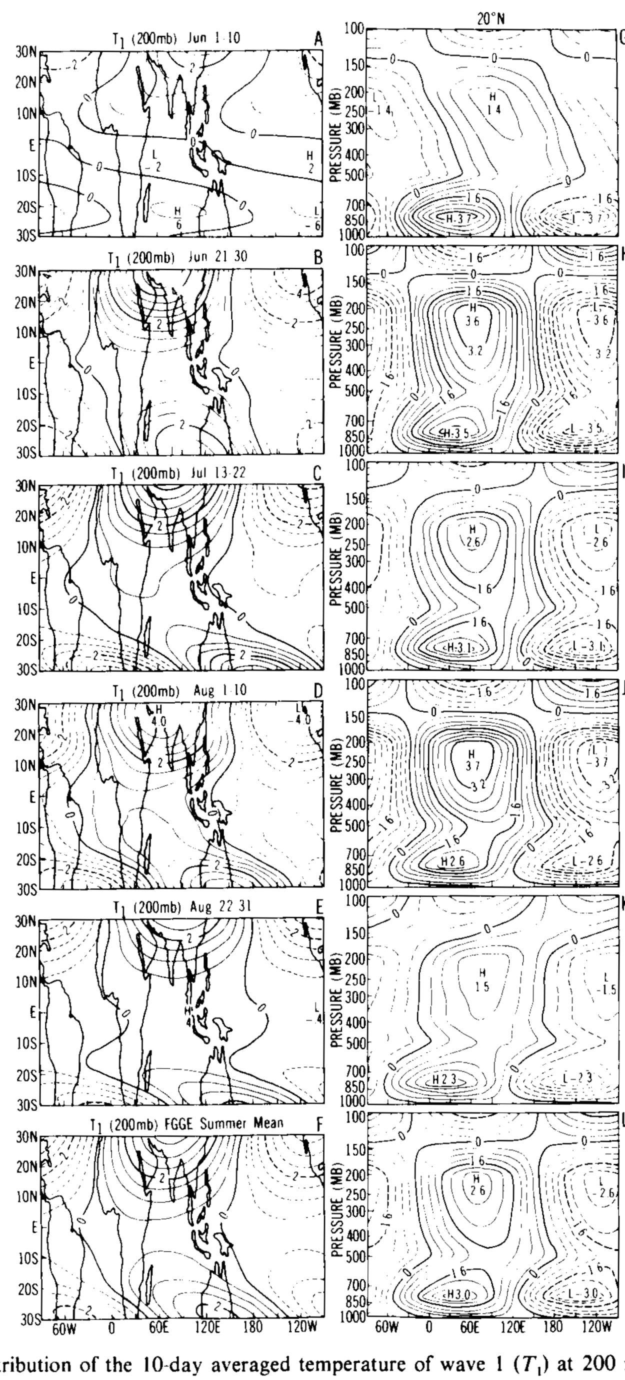

Fig. 9. Horizontal distribution of the 10-day averaged temperature of wave 1 (T_1) at 200 mb (first colum) and the corresponding longitude-pressure cross sections of T_1 at 20° N (second column) for (a) and (g) June 1–10, (b) and (h) June 21–30, (c) and (i) July 13–22, (d) and (j) August 1–10, (e) and (k) August 22–31, and (f) and (1) 1979 summer mean.

state, except in the preonset of monsoon circulation. At this state, the maximum amplitude of wave 1 at 200 mb is much smaller and a westward tilting appears above 500 mb, which is consistent with the NE–SW tilting shown in the horizontal structure at 200 mb. The time variation of amplitude is more significant in the upper troposphere than is the lower troposphere. It was also shown (Chen and Marshall, 1984) that the eddy (or wave 1) available potential energy displays a bimodal vertical distribution with the major maximum value in the upper troposphere. The contrast of amplitude in the time variation between the upper and lower troposphere indicates that the OHM variation of the eddy-available potential energy is mostly attributed to the former region.

4.2.2. Zonal velocity. The zonal wind structure of wave 1 (u_1) is depicted in Fig. 10. The summer-mean state at 200 mb (Fig. 10f) shows that the westward motion ($u_1 < 0$) exists in the monsoon area and the eastward motion ($u_1 > 0$) appears outside this area. The contrast between Figs. 9 and 10 indicates that the former is associated with the thermal ridge of wave 1 and the latter with the thermal trough of this wave in the tropics. The tropical easterly jet core is generally situated over the southern Indian subcontinent. Since the maximum westward zonal motion of wave 1 is close to this area, it suggests that wave 1 is an important ingredient forming this jet. The distribution of summer-mean u_1 between the equator and 20° S is very similar to that of the summer-mean eddy zonal motion in our recent study for the standing eddy in the summer tropics. It was found that the summer-mean eddy zonal motion in this area is essentially supported by interactions with the zonal flow and transient eddies. In contrast, the summer-mean zonal eddy motion north of the equator is maintained by the release of available potential energy of the summer-mean eddies. In other words, the time-mean eddy motions north and south of the equator are driven by different mechanisms.

The time evolution in the zonal motion of wave 1 (Figs. 10a–e) shows that the OHM variation originates from two areas around 10° S and 20° N where maximum u_1 appears at the same time. Although the zonal motion of wave 1 during these two phases of maximum eddy energies has a structure similar to the summer-mean state, the maximum u_1 at 20° N is more stationary in its location. The difference in mobility of wave 1 may also imply a difference in the structure and maintenance mechanism of u_1 between these two areas.

The time evolution in the u_1 vertical structure at 20° N (Figs. 10a–k) does not display a significant east-west movement. This situation is consistent with what was shown by the Hovmöller diagrams. The maximum time variation of u_1 always occurs in the upper troposphere. At 10° S, the u_1 vertical structure in the preonset of monsoon and the last phase of minimum eddy energies differs from that of the time-mean eddy to a significant degree. The maximum amplitude of u_1 descends down to 300 mb during these two phases. In other words, the OHM variation of u_1 south of the equator occurs not only in its amplitude, but also in the altitude of maximum amplitude.

5. Dynamic transport properties of wave 1

It is inferred from the structure that the dynamics of wave 1 in the areas north and south of the equator may be different, and in turn, the maintenance of the OHM variation of tropical energetics in these areas should also be different. The vertical sensible heat transport is related to the release of eddy-available potential energy by the thermally direct overturnings, while the horizontal momentum transport is in association with the exchange of kinetic energy between the zonal and eddy flows. These two transport processes of wave 1 will be used to illustrate how the OHM variation is maintained following the presentation of the wave 1 structure shown in Section 4.

5.1. *Vertical transport of sensible heat*

It was shown in Fig. 3 that the OHM variation in the release of eddy-available potential energy, $C(A_E, K_E)$, is dominated by wave 1, $C(A_1, K_1)$. Since the release of available potential energy is evaluated in terms of the vertical sensible heat transport, the OHM variation in $C(A_E, K_E)$ (or $C(A_1, K_1)$) may be mainly decided by the vertical sensible heat transport of wave 1, $\omega_1 T_1$. Furthermore, the summer-mean vertical distribution of $C(A_1, K_1)$ has its maximum value at 200 mb. The horizontal distribution of $\omega_1 T_1$ at this level for various phases of the tropical energetics is dis-

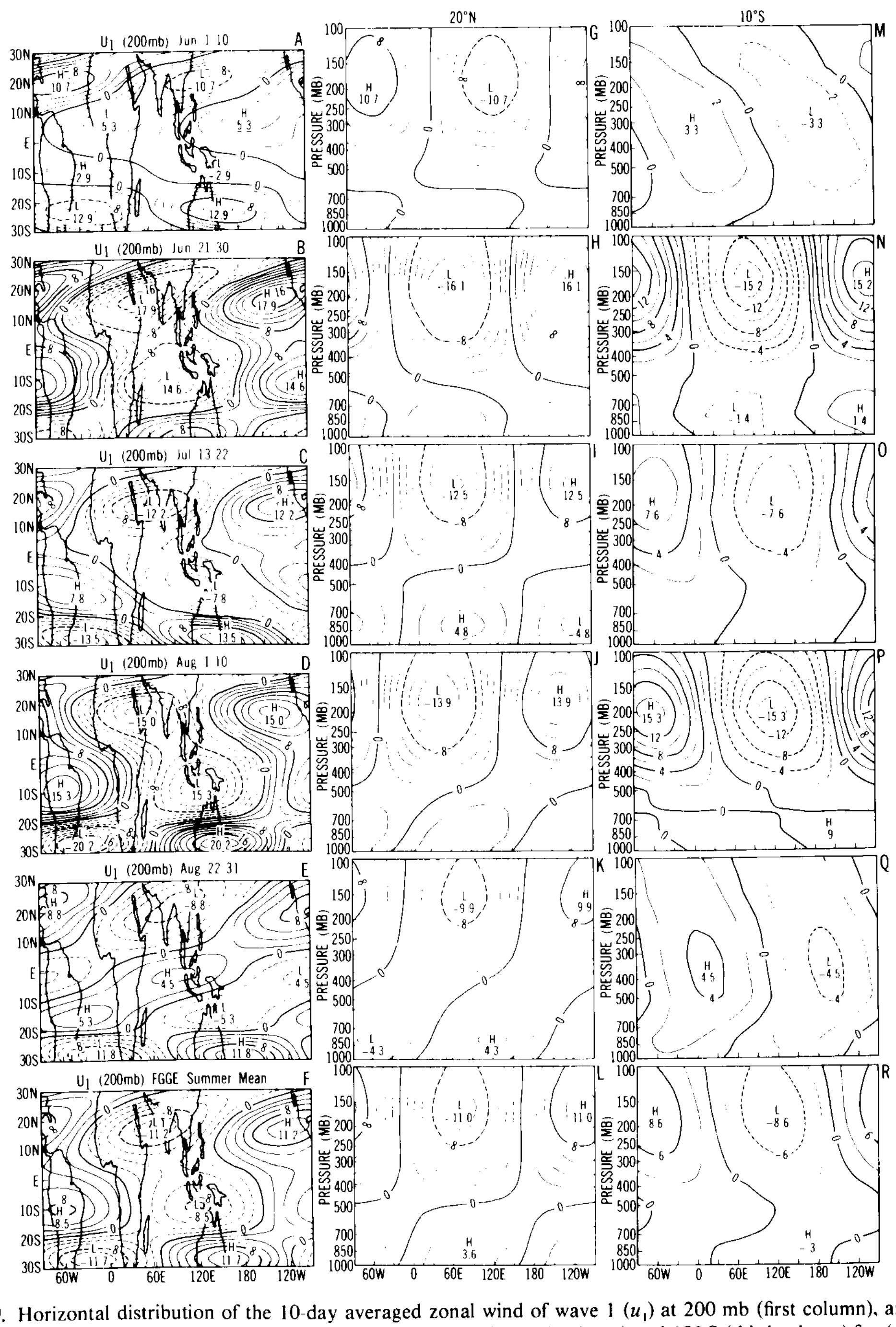

Fig. 10. Horizontal distribution of the 10-day averaged zonal wind of wave 1 (u_1) at 200 mb (first column), and the corresponding longitude-pressure cross sections of u_1 at 20° N (second column) and 10° S (third column) for (a), (g), (m) 1–10, (b), (h), (n) June 21–30, (c), (i), (o) July 13–22, (d), (j), (p) August 1–10, (e), (k), (q) August 22–31, and (f), (l), (r) 1979) summer mean.

played in Figs. 11a–e. It is evident that $\omega_1 T_1$ is significant in the area north of the equator when the eddy energies reach their maximum values. The vertical distribution of $\omega_1 T_1$ at 20° N during the corresponding phases of the tropical energetics is also shown in Figs. 11f–j. $\omega_1 T_1$ is significant over the entire troposphere north of the equator when the eddy energies are maximum.

Eqs. (2) and (4) indicate that the release of available potential energy by wave 1 is a source of kinetic energy and a sink of available potential energy of this wave. The geographic distribution of $\omega_1 T_1$ and time variation in magnitude coincides with those of temperature and zonal motion of wave 1 in the area north of the equator. It suggests that the kinetic energy of wave 1 (K_1) responds to the time variation in the available potential energy of wave 1 (A_1) through $C(A_1, K_1)$. Eq. (4) also

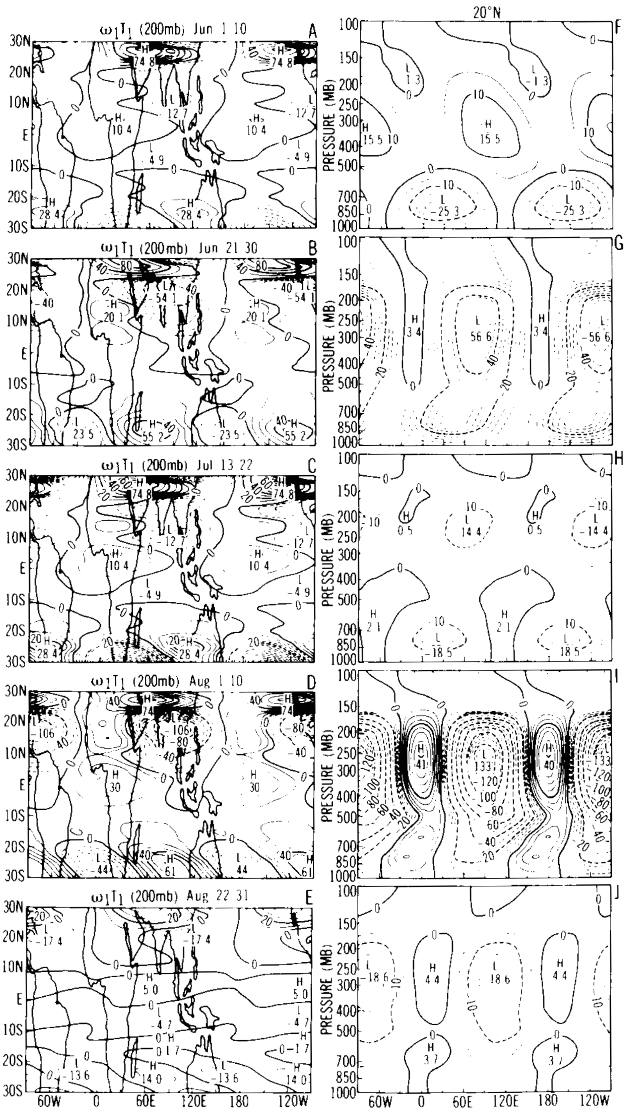

Fig. 11. Horizontal distribution of the vertical sensible heat transport of wave 1 ($\omega_1 T_1$) at 200 mb (first column) and longitude-pressure cross sections of $\omega_1 T_1$ at 20° N (second column) for (a) and (f) June 1–10, (b) and (h) June 21–30, (c) and (i) July 13–22, (d) and (j) August 1–10, (e) and (k) August 22–31. Units: 10^{-7} degree mb s^{-1}.

indicates that the generation of available potential energy, $G(A_1)$, the exchange between zonal and wave-1 available potential energy, $C(A_Z, A_1)$, and the non-linear transfer process, $CA(1/m, l)$, may be possible sources of A_1. It was shown in Fig. 6 that the numerical value of the non-linear transfer process is small in the tropics. The horizontal sensible heat transport of wave 1 (not shown) is only significant poleward of 20° N over most of the summer. Since the north-south temperature gradient in the tropics is small, it may not be expected that $C(A_Z, A_1)$ plays a significant rôle supporting A_1. Another possible mechanism supplying A_1 is the generation process, $G(A_1)$, which involves the diabatic heating of wave 1. At any rate, the pursuit of this matter is beyond the scope of the present study and suggests a further effort in the future.

Recall that the temperature amplitude of wave 1 in the area south of the equator is not significant. It is inferred that no significant available potential energy of wave 1 can be released to support the atmospheric motion in this area. The negligible magnitude of $\omega_1 T_1$ confirms this argument. In view of this reasoning, a different physical process may exist to maintain the atmospheric motion here.

5.2. *Horizontal transport of momentum*

Eq. (2) shows that the kinetic energy of wave 1 (K_1) can be supplied by three sources: release of available potential energy by this wave, $C(A_1, K_1)$, exchange of kinetic energy between wave 1 and zonal flow $C(K_1, K_Z)$, and non-linear exchange of kinetic energy between wave 1 and other waves, $CK(1/m, l)$. It was illustrated previously that $C(A_1, K_1)$ is insignificant south of the equator, and $CK(1/m, l)$ serves to transfer kinetic energy out of wave 1. Another possible source supporting K_1 is $C(K_1, K_Z)$. Note that this energy exchange was shown to be a small positive value in Section 3. One may question what would be the energy source maintaining the motion of wave 1 in the area south of the equator. Our recent energetics study of the tropical atmosphere indicates that the north–south wind shear of the mean zonal flow changes its sign in the region between the equator and 10° N, where the maximum easterly is located. The horizontal momentum transport by wave 1 in the upper troposphere is usually northward on both sides of the equator during the FGGE summer. Therefore, the numerical value of $C(K_1, K_Z)$ changes its sign as the north–south wind shear of the mean zonal flow does. If we examine only one side of the maximum easterly, $C(K_1, K_Z)$ is negative in the south side and positive in the north side, especially in the upper troposphere. In light of these arguments, the cancellation of positive and negative values in the latitudinal integration of $C(K_1, K_Z)$ in the tropics results in a small value for this energy conversion.

It was observed that the north–south wind shear (not shown), especially in the upper troposphere, does not vary significantly in time south of the equator. The extraction of kinetic energy from zonal flow to support wave 1 south of the equator is determined by the momentum transport of wave 1. The horizontal distributions of the 10-day averaged $u_1 v_1$ at 200 mb in various phases of the tropical energetics are depicted in Figs. 12a–e. The momentum transport by wave 1 becomes significant, particularly south of the equator, when eddy energies reach their maximum values. The vertical cross sections of $u_1 v_1$ at 10° S are also exhibited in Figs. 12f–j for the corresponding phases as the horizontal distribution of $u_1 v_1$. The momentum transport is always negligible in the lower troposphere, but becomes very intense in the upper troposphere when eddy energies peak their values. The monsoon area experiences the maximum northward momentum transport during these particular phases.

The time variation of $u_1 v_1$ indicates that $C(K_1, K_Z)$ has its maximum value and its maximum OHM variation in the upper troposphere. Recall that the OHM variation in the eddy kinetic energy essentially occurs in the upper troposphere. It is inferred that this OHM variation in the eddy kinetic energy south of the equator is consistent with that of the barotropic energy exchange not only in time, but also in the spatial location.

6. Concluding remarks and discussion

The temperature and wind fields generated by the FGGE III-b analyses of the European Center for Medium Range Weather Forecasts (ECMWF) are used to examine the time variation of the tropical energetics during the FGGE summer. The eddy-available potential and kinetic energies, and some energy conversions exhibit a pronounced quasi-periodic variation with a period of $1\frac{1}{2}$ months

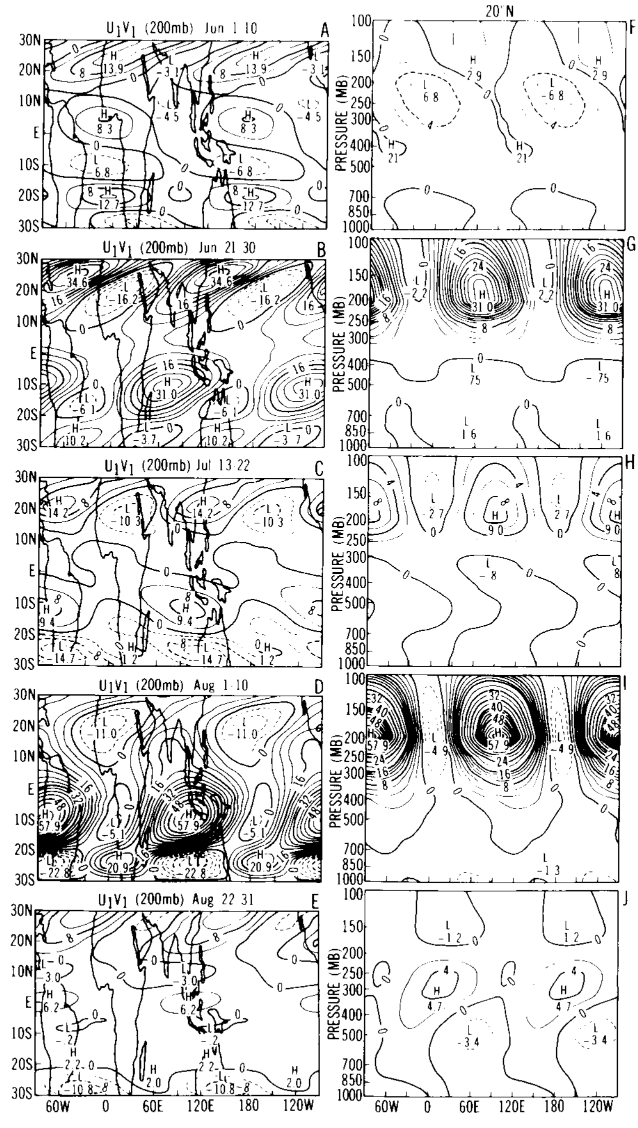

Fig. 12. Horizontal distribution of the momentum transport of wave 1 (u_1v_1) at 200 mb (first column) and longitude-pressure cross sections of u_1v_1 at 10° S (second column) for (a) and (f) June 1–10, (b) and (h) June 21–30, (c) and (i) July 13–22, (d) and (j) August 1–10, (c) and (j) August 22–31. Units: $m^2 s^{-2}$.

(OHM). It was found that this OHM variation in the tropical energetics is essentially due to wave 1. The eddy available potential energy is evaluated from the variance of temperature disturbances, while the eddy kinetic energy is mainly attributed to the zonal motion. In order to facilitate the search for the possible mechanism inducing and maintaining the OHM variation in the tropical energetics, an effort was made to examine the energetics, propagation, time evolution in the three-dimensional structure, and dynamical transport of wave 1 in terms of temperature and zonal motion.

The spectrally-filtered (SF) Hovmöller diagrams at 10° S and 20° N, and latitude (30° S–30° N)-time diagrams of the root-mean-square amplitude for the temperature and zonal wind of wave 1 over the entire FGGE summer are used to explore the mobility of this wave. Our attention focuses on the 200-mb level because the OHM variation in the tropical energetics essentially occurs in the upper troposphere. Wave 1 seems to be quasi-stationary north of the equator and moves slowly eastward south of the equator. This wave is amplified roughly in about the same location. The likely eastward movement of the transient mode of wave 1 may be consistent with Madden and Julian's (1971) finding of a 40–50 day oscillation in the zonal wind and surface pressure over the tropics. It was later suggested by Madden and Julian (1972) that this oscillation is due to an eastward movement of global-scale circulation cells oriented in the equatorial (zonal) plane. The maximum intensity of this oscillation occurs in the central Pacific. The eastward propagation of the transient mode of wave 1 may be perceived by removing its summer time-mean mode in the SF Hovmöller diagrams.

Yasunari (1979, 1980, 1981) also found a 40–50 day oscillation in his analyses of cloudiness and other meteorological variables over the northern Indian Ocean. This oscillation migrates northward from 10° S to 20° N. Based upon the analyses of 850-mb wind field, Krishnamurti and Subrahmanyam (1982) also reported a 40–50 day oscillation in the summer monsoon area. They found that a train of troughs and ridges associated with the 40–50 day variation is formed around the equator. It moves northward and dissipates near the Himalayas. In the present study, wave 1 at 200 and 850 mb (not shown) does not provide strong evidence of northward movement. In fact, the east–west extent of the disturbances discussed by Yasunari or Krishnamurti and Subrahmanyam is much smaller than wave 1. At any event, whether there is any link relating the 40–50 day oscillation of those studies to the OHM variation in the tropical energetics of the FGGE summer is worth pursuing.

The time evolution in the 3-dimensional structure of wave 1 indicates that the OHM variation in the eddy-available potential energy mainly exists north of the equator and the OHM variation in the eddy kinetic energy originates from areas both north and south of the equator. The structure and dynamical transport properties of wave 1 show that the OHM variation in the tropical energetics north and south of the equator are maintained by different mechanisms. In the area north of the equator, the OHM variation in the eddy kinetic energy is supported by the release of eddy-available potential energy. It was also argued that the OHM variation in the eddy-available potential energy is maintained by the generation of eddy-available potential energy, which is evaluated in terms of the covariance between the diabatic heating and temperature perturbation of wave 1. One may wonder *what* and *where* the possible mechanism causing the OHM variation in diabatic heating would be. The positive temperature perturbation of wave 1 and the observations of cloudiness and rainfall suggest that the strong diabatic heating due to the latent heat release of cumulus convection occurs over the summer monsoon area. Yasunari (1981) proposed a schematic model describing the 40–50 oscillation of the anomalous Hadley circulation. In this model, the cumulus convection starts at the equator where the upward branch of Hadley circulation is located. The cumulus convection associated with this upward branch of Hadley circulation moves northward and obtains its maximum intensity at 20° N. The cumulus convection finally dies out when it reaches the Himalyas. The entire life cycle of this northward migration is about 40 days. The general picture of Yasunari's is consistent with the northward migration of the trough line at 850 mb over the north Indian Ocean during the monsoon season described by Krishnamurti and Subrahmanyam (1982). Furthermore, an interesting feature was also revealed in the comparison between the time series of eddy energies and the migration of trough and ridge line in Krishnamurti and Subrahmanyam's synoptic analysis. The eddy energies were at a minimum when the ridge line reaches the Himalayas before the onset of monsoon. In contrast, the eddy energies became maximal when the trough line arrives at the Himalayas. It seems that the latent heat released by the cumulus convection migrating with the trough line from the equator to the Himalayas is a possible mechanism responsible for the OHM variation in the generation of eddy-available potential energy.

In the area south of the equator, it is observed that the north-south zonal wind shear in the upper troposphere does not vary significantly with time. The momentum transport by wave 1 varies with the eddy kinetic energy. It is inferred that the extraction of the kinetic energy from zonal flow to support the kinetic energy of wave 1 south of the equator is in concert with the time variation of energetics intensity north of the equator. In other words, the OHM variation in the eddy kinetic energy south of the equator is maintained by the barotropical conversion from zonal kinetic energy. However, what mechanism synchronizes the OHM variation in the atmospheric energetics of the tropics north and south of the equator imposes a challenging problem for further investigation.

As mentioned previously, the understanding of the mechanism causing the OHM variation in the tropical energetics may be important to the long-range weather forecast or short-term climate prediction in the tropics. Although some mechanisms were suggested above, it does not mean that the OHM variation in the tropical energetics is well understood. The diagnostic analysis of the present study only indicates some direction for further effort.

7. Acknowledgement

This study was supported jointly by the National Science Foundation and the National Oceanic and Atmospheric Administration under the Grant ATM-8206789. The major computation was performed on the CRAY-1 computer of the National Center for Atmospheric Research which is sponsored by the National Science Foundation. Dr. Hal G. Marshall provided help at the initial stages of this study and Mr. John G. Vorwald completed the computation. The suggestions from Drs. Roland A. Madden and Joseph J. Tribbia are appreciated. Comments offered by referees significantly improved the presentation of this paper.

REFERENCES

Bengtsson, L., Kanimitsu, Kolloberg, P. and Uppala, S. 1982. FGGE 4-dimensional data assimilation at ECMWF. *Bull. Am. Meteorol. Soc. 63*, 29–43.

Chen, T.-C. 1980. On the exchange between the divergent and rotational components of atmospheric flow over the tropics and subtropics at 200 mb during two northern summers. *Mon. Wea. Rev. 108*, 896–912.

Chen, T.-C. 1983. The energy exchange between the baroclinic and barotropic components of atmospheric flow in the tropics during the FGGE summer. *Mon. Wea. Rev. 111*, 1389–1396.

Chen, T.-C. and Marshall, H. G. 1984. Time variation of atmospheric energetics during the FGGE winter. *Tellus 36A*, 251–268.

Chen, T.-C. and Buja, L. E. 1983. A comparison study for the time variation of the atmospheric energetics between two hemispheres during the FGGE year: annual variation and vacillation. Preprints from *the First Conference on Southern Hemisphere Meteorology*, July 31-August 6, 1983, Sao Jose Dos Campos, Brazil. American Meteorological Society.

Chen, T.-C. and Marshall, H. G. 1984. A further study on the atmospheric energetics of large-scale motions in the tropics. Technical report, Department of Earth Sciences, Iowa State University, Ames, IA, USA, pp. 28 (available from the author).

Depradine, C. A. 1980. Energetics of large-scale motion in the tropics during GATE at 250 mb. *Mon. Wea. Rev. 108*, 886–895.

Hunt, B. G. 1978. Atmospheric vacillation in a general circulation model (I). The large-scale energy cycle. *J. Atmos. Sci. 35*, 1133–1143.

Kanamitsu, M., Krishnamurti, T. N. and Depradine, C. 1971. On scale interaction in the tropics during northern summer. *J. Atmos. Sci. 29*, 698–706.

Krishnamurti, T. N. 1979. Large-scale feature of the tropical atmosphere. In: *Meteorology of the tropical oceans*, ed. D. B. Shaw. *Roy. Met. Soc.*, 31–56.

Krishnamurti, T. N. and Bhalme, H. N. 1976. Oscillation of a monsoon system. Part I. Observational aspects. *J. Atmos. Sci. 33*, 1937–1954.

Krishnamurti, T. N. and Subrahmanyam, D. 1982. The 30–50 day mode at 850 mb during MONEX. *J. Atmos. Sci. 39*, 2088–2095.

Madden, R. A. and Julian, P. R. 1971. Detection of a 40–50 day oscillation in the zonal wind in the tropical Pacific. *J. Atmos. Sci. 28*, 702–708.

Madden, R. A. and Julian, P. R. 1972. Description of global-scale circulation cells in the tropics with a 40–50 day period. *J. Atmos. Sci. 29*, 1109–1123.

O'Brien, J. J. 1970. Alternative solutions to the classical vertical velocity problem. *J. Appl. Meteorol. 9*, 197–203.

Rao, M. S. V. and Theon, J. S. 1977. New features at global climatology revealed by satellite-derived oceanic rainfall maps. *Bull. Amer. Meteorol. Soc. 58*, 1285–1288.

Sadler, J. C. 1969. *Average cloudiness in the tropics from Satellite Observation.* East-West Center Press, University of Hawaii, Honolulu, 22 pp.

Saltzman, B. 1957. Equations governing the energetics of the large-scales of atmospheric turbulence in the domain of wavenumber. *J. Meteorol. 14*, 513–529.

Sela, J. and Wiin-Nielsen, A. 1971. Simulation of the atmospheric annual energy cycle. *Mon. Wea. Rev. 99*, 460–468.

White, G. H. 1982. An observational study of the northern hemisphere extratropical summer time general circulation. *J. Atmos. Sci. 39*, 24–40.

Wiin-Nielsen, A. 1967. On the annual variation and spectral distribution of atmospheric energy. *Tellus 19*, 540–559.

Yasunari, T. 1979. Cloudiness fluctuations associated with the northern hemisphere summer monsoon. *J. Meteorol. Soc. Japan 57*, 227–242.

Yasunari, T. 1980. A quasi-stationary appearance of 30 to 40 day period in the cloudiness fluctuations during the summer monsoon over India. *J. Meteorol. Soc. Japan 58*, 225–229.

Yasunari, T. 1981. Structure of an Indian summer monsoon system with around 40-day period. *J. Meteorol. Soc. Japan 58*, 336–354.